Large-angle adjustable coherent atomic beam splitter by Bragg scattering

Please check the document version of this publication:

• A submitted manuscript is the version of the article upon submission and before peer-review. There can be important differences between the submitted version and the official published version of record. People interested in the research are advised to contact the author for the final version of the publication, or visit the DOI to the publisher's website.
• The final author version and the galley proof are versions of the publication after peer review.
• The final published version features the final layout of the paper including the volume, issue and page numbers.

[Link to publication](#)

Large-angle adjustable coherent atomic beam splitter by Bragg scattering

A. E. A. Koolen, G. T. Jansen, K. F. E. M. Domen, H. C. W. Beijerinck, and K. A. H. van Leeuwen*

Eindhoven University of Technology, P.O. Box 513, 5600MB Eindhoven, The Netherlands

Using a ''monochromatic'' (single-axial-velocity) and slow (250 m/s) beam of metastable helium atoms, we realize up to eighth-order Bragg scattering and obtain a splitting angle of 6 mrad at low laser power (3 mW). This corresponds to a truly macroscopic separation of 12 mm on the detector. For fifth-order scattering, we have observed several oscillations of the splitting ratio when varying the laser power (''Pendellösung oscillations''). The large splitting angle, the adjustable splitting ratio, and the cleanness of the split beams, with 200-μm rms width each, make the beam splitter ideal for a large-enclosed-area atom interferometer.

As essential elements for atom interferometers, a large variety of coherent atomic beam splitters and mirrors has been proposed and constructed. Experimentally realized devices include splitters based on diffraction from free standing transmission structures [1,2], the magnetic Stern-Gerlach effect [3], splitting with running waves [4] or by stimulated Raman transitions [5–7], the optical Stern-Gerlach effect [8], a magneto-optical beam splitter [9], diffraction from a blazed phase grating [10], and splitting by an evanescent standing wave [11].

Among the conceptually and experimentally simplest devices are beam splitters based on Bragg scattering of atoms from standing light waves [12]. Bragg scattering for atoms can be described as a multiphoton Raman process, in which an atom with an initial momentum of $p_N = N\hbar k$, with k the wave number of the light, in the direction of the light beams exits in a superposition of the initial momentum state and the state with momentum $p_{-N} = -N\hbar k$. The integer N is the order of the Bragg scattering, and obviously $2N$ photons are exchanged between the atom and the light field. Clean Bragg scattering, where no other momentum states are occupied after the interaction, requires the light field as observed by the atoms to be turned on and off adiabatically.

Bragg beam splitters have both been studied extensively [13–20] as such and have been used to construct atom interferometers [21,22]. In all these experiments (except for the experiments on Bose-Einstein condensate splitting [20,22]), thermal atomic beams are used. Up to sixth order, Bragg scattering has been observed in these experiments [13,20]. However, the beams are split by a fixed transverse momentum and not by a fixed angle. Thus, the spread in axial velocity of the atomic beam causes the diffraction orders to overlap at these high orders. Also, the interaction time dependent effects such as the Pendellösung oscillation [17,18] of the splitting ratio are masked by the spread in interaction time associated with the axial velocity distribution. In order to cleanly separate the higher diffraction orders and fix the interaction time, a ''monochromatic'' (single-axial-velocity) atomic beam has to be used.

In our setup we produce a monochromatic, bright, and extremely well-collimated atomic beam of metastable helium atoms. Figure 1 displays a schematic diagram of the setup. The source is a discharge-excited, liquid-nitrogen-cooled supersonic expansion. The beam is next collimated by two-dimensional (2D) laser cooling, slowed in a Zeeman slower, prefocused by a magneto-optic lens, and compressed by a magneto-optic funnel. The design of the beam setup is described extensively elsewhere [23]. After the compression stage, the beam first passes a 60-μm square aperture and a 25-μm-diameter round aperture, separated by 2 m. After the second aperture we get 250 atoms per second in the metastable state. Optimally, the atoms are 95% spin polarized in the $m = -1$ magnetic substate; however, in the experiments described below 75% of the atoms were in the $m = -1$ state and 25% in the $m = 0$ state. The axial velocity is 247 m/s with an rms spread of 3.7 m/s. The spread in transverse velocity, as measured with a position-sensitive multichannel plate detector 2 m downstream of the second aperture, is 9×10^{-3} m/s. This equals one tenth of the recoil induced by emission or absorption of a single photon at the $\lambda = 1083$-nm transition. Monochromaticity, extreme collimation, and relatively high flux make this beam setup a unique apparatus for studying atom optics in the de Broglie wave regime: The beam can be considered as a plane, nearly monochromatic matter wave when interactions with 1083-nm light are studied.

Immediately after the second aperture, the atomic beam intersects a standing light wave. The light is detuned by -180 MHz with respect to the optical transition, and circularly polarized to excite the ${}^3S_1(m = -1) \rightarrow {}^3P_2(m = -2)$ transition, which has the largest transition strength. The detuning is sufficient to suppress spontaneous emission during the interaction time largely (but not completely). The angle between light wave and atomic beam is adjustable.

The waist of the Gaussian light beam is 850 μm, large enough to ensure that the scattering is in the Bragg- or thick-grating regime. The standing light wave is produced by retroreflection of the beam of a distributed Bragg reflector diode laser. The maximum intensity of this beam after transport through an optical fiber is 3 mW. Two meters downstream of the interaction region, a triple multichannel plate detector with a resistive anode provides position-
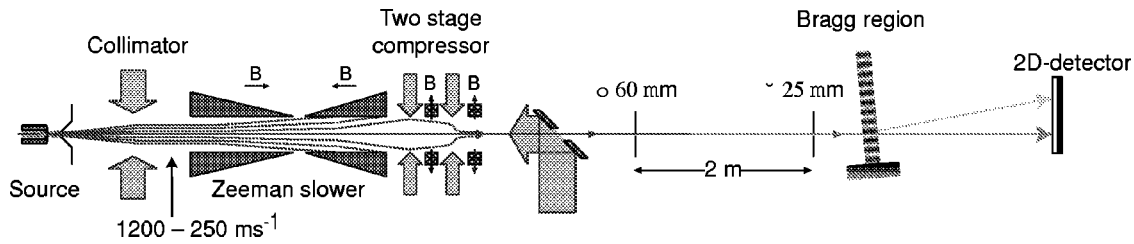
FIG. 1. Schematic diagram of experimental setup.

sensitive detection of individual metastable helium atoms with 60-μm rms resolution.

The low axial velocity of the atoms ensures the adiabatic turn on and turn off of the light field for the passing atoms. The long resulting interaction time enables high-order Bragg diffraction to be observed despite the small available laser power. The order of the Bragg scattering can be determined by tuning the angle of incidence θ_{inc} between the atomic beam axis and the phase planes of the standing light wave. For first-order Bragg scattering, $\theta_{inc} = 0.37$ mrad. As long as consecutive diffraction orders do not merge on the 2D detector and one can produce a sufficiently high intensity of the standing light wave, the Bragg scattering order N can be increased. These measurements are shown in Fig. 2. Each detector image contains 25 000 atoms. The area of each bin is $0.10\hbar k \times 0.10\hbar k$. The gray scale ranges are different for each individual image. They are scaled to the bin with the highest number of atoms.

For $1 \leq N \leq 5$, the intensity of the reflected (p_{-N}) beam was maximized by adjusting the laser power. Ideally, for this choice of laser power the interaction should correspond to an effective π pulse for the $2N$ photon transition and the intensity of the transmitted (p_N) beam should be zero. Figure 2 shows that this is not the case. This is caused by the presence of the 25% $m=0$ atoms (as determined from Stern-Gerlach measurements), which are less effectively scattered due to the lower Clebsch-Gordan coefficient for the $^3S_1(m=-1) \rightarrow {}^3P_2(m=-2)$ transition.

The maximum laser power $P_{L,\max} = 3$ mW prevents us from providing an effective π pulse for $N > 5$. Thus, beam splitters with approximately equal transmission and reflection are made for sixth-, seventh-, and eighth-order Bragg scattering. This gives a maximum splitting angle of 5.9 mrad between both ports of the beam splitter. With an atomic beam diameter of 25 μm the atom only has to travel 4.2 mm before both momentum states of the coherent superposition are spatially separated. On the detector, the atoms are then separated by 12 mm.

Since the diffracted beam stays well within its own diffraction order on the 2D detector, even for eighth-order Bragg scattering, we could in principle go further if we had more laser power. The width of the eighth-order diffraction peak on the 2D detector is 203-μm rms. This is still considerably smaller than the projection of $\hbar k$ on the detector, which is 760 μm. The incoming momentum state produces a 98-μm rms peak on the detector. Note that the real width of the beams is actually smaller because of the finite detector resolution. Extrapolating these results one could theoretically go up to 34th-order Bragg scattering before diffraction orders

start to overlap. This would produce a 25 mrad angle between the two output ports! To achieve full reflection in 34th-order with comparable probability for spontaneous emission would, in the present setup, require a laser power of 1.4 W at a detuning of 8 GHz. This is achievable by inserting a fiber amplifier in the setup.

For fifth-order scattering we studied the Pendellösung effect in atomic Bragg scattering, i.e., the oscillation of the occupation of the two possible final momentum states as a function of interaction strength or time, in detail. So far, this effect has been studied in first- and second-order scattering by Rempe and co-workers [17–19]. The effect can be understood as a Rabi oscillation between two states coupled effectively by a $2N$ photon transition, or alternatively as an adiabatic scattering problem in an atomic Bloch state description. The latter approach provides more insight and will be treated in detail in a forthcoming publication. Figure 3 shows the experimental data as individual detector images for increasing laser power.

The oscillation is clearly visible in this figure. In Fig. 4 the contents of the peaks corresponding to the transmitted and reflected beam are shown as a function of laser power. Some population in the "forbidden" diffraction peaks
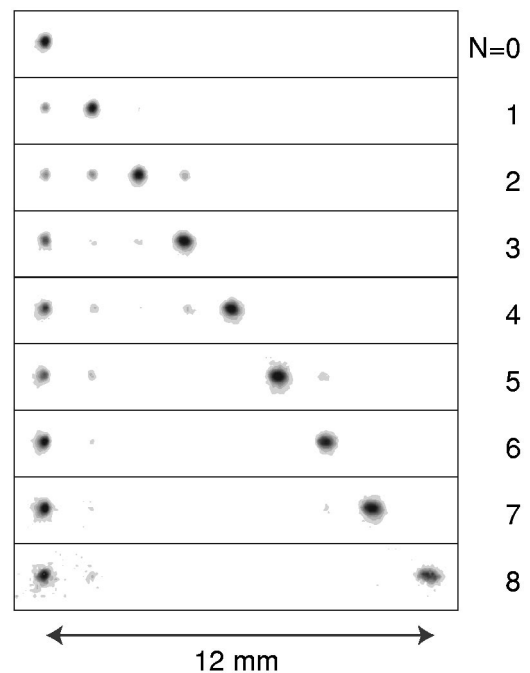
FIG. 2. Bragg scattering for increasing order N. Each image contains 25 000 atoms distributed over $0.10\hbar k \times 0.10\hbar k$ sized bins.
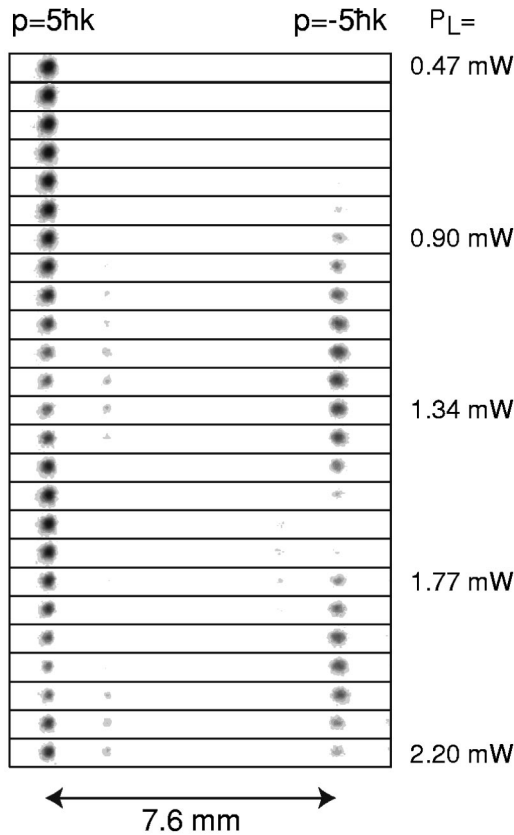
FIG. 3. Pendellösung oscillations in fifth-order Bragg scattering. Each image contains 10 000 atoms distributed over $0.07\hbar k \times 0.07\hbar k$ sized bins. The incoming momentum state has momentum $5\hbar k$ and the Bragg diffracted state momentum $-5\hbar k$ along the direction of the light beams.
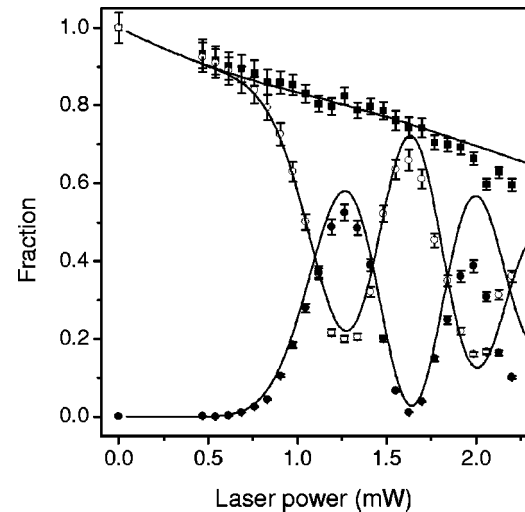

FIG. 4. Pendellösung oscillations in fifth-order Bragg scattering. The measured occupation of the incoming state with momentum $=5\hbar k$ (open circles) and the Bragg diffracted state with momentum $-5\hbar k$ (filled circles) are shown as a function of the laser power. The total coherent fraction is given by the filled squares. The decrease in this fraction with increasing laser power is caused by spontaneous emission. The solid lines are the calculated curves for a vertical mismatch between the atomic beam and the center of the laser beam of 0.46 mm.

(hardly visible in Fig. 3) is also detected. This is probably due to nonadiabatic transitions caused by wave front imperfections in the standing light wave. The total population in all diffraction peaks is also shown in Fig. 4. The apparent loss in the normalization with increasing laser power is caused by the atoms that undergo spontaneous emission during the interaction. These atoms are detected, but generally do not end up in the diffraction peaks due to the random recoil induced by the spontaneously emitted photon. The results of a calculation based on the numerical integration of the time dependent Schrödinger equation describing the atom in the light field is shown as well. The calculation takes the internal as well as external (center-of-mass motion) states of the atom into account. Spontaneous emission is incorporated as a decay term in the Hamiltonian. The initial magnetic substate distribution is set to 75% in $m=-1$ and 25% in $m=0$ atoms. The offset in the alignment of laser and atomic beam, which accounts for an effective decrease in peak light intensity, is the only adjustable parameter. The calculation is seen to reproduce the experimental results excellently.

The present results, which demonstrate the splitting of an atomic beam in two parts with a truly macroscopic separation, can be used to construct an atom interferometer with a very large enclosed area. Using three Bragg zones, the first and last set to 50-50 splitting, with the middle one set to 100% reflection, a Mach-Zehnder interferometer is realized [13]. Using tenth-order Bragg scattering, which is easily attainable by using more laser power, a maximum splitting of 6 mm in the middle of the existing 2 m length between the final collimating aperture and the detector, and an enclosed area of 5400 mm^2 between the arms can be reached. This should be compared to existing atom beam interferometers, which have maximum beam separations of up to 60 μm and enclosed areas of up to 40 mm^2. This would not only constitute an interferometer with a potentially very large sensitivity for, e.g., rotation measurements [24], but more importantly would allow a large variety of interferometric measurements where the macroscopic separation between the two arms is essential. The latter can include measurements where both arms pass through separate optical cavities for cavity QED studies, and measurements where the influence of fields *in between* the two arms is studied (Aharonov-Bohm related topological phases). We are at present busy constructing such a general-purpose very-large-area atom interferometer.

[1] O. Carnal and J. Mlynek, Phys. Rev. Lett. **66**, 2689 (1991).

[2] D.W. Keith, C.R. Ekstrom, Q.A. Turchette, and D.E. Pritchard, Phys. Rev. Lett. **66**, 2693 (1991).

[3] C. Miniatura, J. Robert, S.L. Boiteux, J. Reinhardt, and J. Baudon, Appl. Phys. B: Photophys. Laser Chem. **54**, 347 (1992).

[4] C.J. Bordé, N. Courtier, F. du Burck, A.N. Goncharov, and M. Gorlicki, Phys. Lett. A **188**, 187 (1994).

[5] M. Kasevich and S. Chu, Phys. Rev. Lett. **67**, 181 (1991).

[6] D.S. Weiss, B.C. Young, and S. Chu, Phys. Rev. Lett. **70**, 2706 (1993).

[7] J.M. McGuirk, M.J. Snadden, and M.A. Kasevich, Phys. Rev. Lett. **85**, 4498 (2000).

[8] T. Sleator, T. Pfau, V. Balykin, O. Carnal, and J. Mlynek, Phys. Rev. Lett. **68**, 1996 (1992).

[9] T. Pfau, C. Kurtsiefer, C.S. Adams, M. Sigel, and J. Mlynek, Phys. Rev. Lett. **71**, 3427 (1993).

[10] K.S. Johnson, A.P. Chu, K.K. Berggren, and M. Prentiss, Opt. Commun. **126**, 326 (1996).

[11] R. Brouri, R. Asimov, M. Gorlicki, S. Feron, J. Reinhardt, V. Lorent, and H. Haberland, Opt. Commun. **124**, 448 (1996).

[12] P.J. Martin, B.G. Oldaker, A.H. Miklich, and D.E. Pritchard, Phys. Rev. Lett. **60**, 515 (1988).

[13] D.M. Giltner, R.W. McGowan, and S.A. Lee, Phys. Rev. A **52**, 3966 (1995).

[14] M.K. Oberthaler, R. Abfalterer, S. Bernet, J. Schmiedmayer, and A. Zeilinger, Phys. Rev. Lett. **77**, 4980 (1996).

[15] S. Bernet, M.K. Oberthaler, R. Abfalterer, J. Schmiedmayer, and A. Zeilinger, Phys. Rev. Lett. **77**, 5160 (1996).

[16] C. Keller, M.K. Oberthaler, R. Abfalterer, S. Bernet, J. Schmiedmayer, and A. Zeilinger, Phys. Rev. Lett. **79**, 3327 (1997).

[17] S. Kunze, S. Dürr, and G. Rempe, Europhys. Lett. **34**, 343 (1996).

[18] S. Dürr, S. Kunze, and G. Rempe, Quantum Semiclassic. Opt. **8**, 531 (1996).

[19] S. Dürr and G. Rempe, Phys. Rev. A **59**, 1495 (1999).

[20] M. Kozuma, L. Deng, E.W. Hagley, J. Wen, R. Lutwak, K. Helmerson, S.L. Rolston, and W.D. Phillips, Phys. Rev. Lett. **82**, 871 (1999).

[21] D.M. Giltner, R.W. McGowan, and S.A. Lee, Phys. Rev. Lett. **75**, 2638 (1995).

[22] Y. Torii, Y. Suzuki, M. Kozuma, T. Sugiura, T. Kuga, L. Deng, and E.W. Hagley, Phys. Rev. A **61**, 041602(R) (2000).

[23] R.M.S. Knops, A.E.A. Koolen, H.C.W. Beijerinck, and K.A.H. van Leeuwen, Laser Phys. **9**, 286 (1999).

[24] T.L. Gustavson, A. Landragin, and M.A. Kasevich, Class. Quantum Grav. **17**, 2385 (2000).